4. Semester Report

Dániel Tibor Pozsár (danielpozsar@ttk.elte.hu)
PhD program: Statistical Physics, Biological Physics and Physics of Quantum Systems
Supervisors: Viktor Ivády, László Oroszlány
Ph.D. Thesis title: Molecular magnets for quantum technology applications

June 23, 2026

Introduction

This report summarizes my work and research on first-principles and many-body computational studies of magnetic and defect-spin systems relevant to quantum technology. Two strands run through the work: (i) the extraction of the parameters of the generalized relativistic Heisenberg Hamiltonian from DFT via the LKAG torque method, implemented in the `grogupy` package, and their use in finite-temperature spin simulations; and (ii) the application of established open-quantum-system theory to simulate the decoherence of optically addressable spin defects in a structured spin bath. During the current semester both principal projects were brought to maturity. The following two sections summarize the results of the first three semesters and then describe the work carried out this semester, emphasizing my own contribution to the multi-author projects.

Summary of the first three semesters

Semester 1: the `grogupy` package and the relativistic exchange formalism

The modeling backbone of the whole project is the generalized relativistic Heisenberg Hamiltonian,

$$H(\{\mathbf{e}_i\}) = \frac{1}{2}\sum_{i\neq j} J_{ij}^{\mathrm{iso}}\,\mathbf{e}_i\cdot\mathbf{e}_j + \frac{1}{2}\sum_{i\neq j}\mathbf{e}_i\,\mathcal{J}_{ij}^{S}\,\mathbf{e}_j + \frac{1}{2}\sum_{i\neq j}\mathbf{D}_{ij}\cdot(\mathbf{e}_i\times\mathbf{e}_j) + \frac{1}{2}\sum_{i}\mathbf{e}_i\,\mathcal{K}_i\,\mathbf{e}_i, \quad (1)$$

where $\mathbf{e}_i$ are unit vectors along the local moments, J_{ij}^{iso} is the isotropic exchange, $\mathcal{J}_{ij}^{S}$ the symmetric anisotropic exchange, $\mathbf{D}_{ij}$ the Dzyaloshinskii–Moriya (DM) vectors and $\mathcal{K}_i$ the single-ion anisotropy. The central difficulty is not the underlying DFT calculation but the systematic and reliable extraction of these tensors from it. I created `grogupy`, a Python library (available on pip) that solves this problem with the Liechtenstein–Katsnelson–Antropov–Gubanov (LKAG) torque method generalized to the non-orthogonal basis sets produced by SIESTA [**soler2002siesta**, 1].

The method expands the total energy to second order in small, site-local rotations of the magnetic moments about an axis $\mathbf{u}_A$. Writing the rotated direction as $\mathbf{o}_A(\theta) = \mathbf{o} + \theta\,\mathbf{o}_A^1 + \frac{1}{2}\theta^2\,\mathbf{o}_A^2 + \ldots$, the first- and second-order energy variations of the spin model read

$$E_A^1(\{\mathbf{o}\}, \mathbf{u}_A) = \frac{1}{2}\left(\mathbf{o}\Big(\sum_i \mathcal{J}_{iA} + 2\mathcal{K}_A\Big)\mathbf{o}_A^1 + \mathbf{o}_A^1\Big(\sum_i \mathcal{J}_{Ai} + 2\mathcal{K}_A\Big)\mathbf{o}\right), \tag{2}$$

$$E_A^2(\{\mathbf{o}\}, \mathbf{u}_A) = \frac{1}{2}\left(\mathbf{o}\Big(\sum_i \mathcal{J}_{iA} + 2\mathcal{K}_A\Big)\mathbf{o}_A^2 + \mathbf{o}_A^2\Big(\sum_i \mathcal{J}_{Ai} + 2\mathcal{K}_A\Big)\mathbf{o}\right) + \mathbf{o}_A^1\mathcal{K}_A\mathbf{o}_A^1. \tag{3}$$

These are matched, order by order, to the corresponding variations of the Kohn–Sham grand potential, which are evaluated from the single-particle Green's function $\hat{G}_0(\epsilon)$ of the converged DFT Hamiltonian — built from the Hamiltonian and the overlap matrix $\hat{S}$ of the non-orthogonal LCAO basis — through the torque expression

$$\delta E_A^{\mathrm{KS}} = -\frac{1}{\pi}\int_{-\infty}^{E_F} d\epsilon\ \mathrm{Im}\,\mathrm{Tr}\ \ln\big(\hat{I} - \hat{V}_A\hat{G}_0(\epsilon)\big), \tag{4}$$

with $\hat{V}_A$ the perturbation generated by the local rotation. Carrying out the energy integration along a contour in the complex plane up to the Fermi level E_F and projecting onto pairs of magnetic entities yields the full set of tensors, including the antisymmetric DM part, which requires spin–orbit coupling, and the symmetric anisotropic part $\mathcal{J}^S$.

Computationally, the method is dominated by repeated evaluations of $\hat{G}_0(\epsilon)$ at many energy points and by the trace over pairs of magnetic entities. `grogupy` represents magnetic entities at several scales — single atoms, atomic shells, or clusters of atoms — and builds the interacting pairs automatically from a real-space interaction cutoff supplemented by user-defined selection rules. The work is distributed across MPI ranks, while the dense Green's-function linear algebra is offloaded to GPUs for the large systems with hundreds of atoms in the unit cell.

The implementation was tested principally on CrI_3. There, the Curie temperature came out around 23 K — roughly half of the value reported in the literature for the monolayer — and we investigated the origin of this discrepancy through bilayer systems, in which the interlayer stacking and coupling strongly influence the ordering temperature. These tests also underlined how important it is, in magnetic materials, to reproduce the crystal symmetry faithfully: the symmetry relates the bonds within and between coordination shells and constrains the allowed components of $\mathcal{J}_{ij}^S$ and $\mathbf{D}_{ij}$, so respecting it both reduces the number of independent tensor elements that must be computed and provides an internal consistency check on the result.

Semester 2: software maturation, triangulenes, and reservoir computing

`grogupy` was matured into a documented Python library distributed on pip, organized around a clean separation between a front end that constructs magnetic entities and pairs and a set of interchangeable numerical backends (dense CPU, MPI, and GPU) selected at runtime; SIESTA input/output is handled through the `sisl` ecosystem. A key addition was the anisotropy-tensor fitting machinery: sampling the energy over many spin rotations and fitting the tensor components, rather than relying on a minimal closed-form set of rotations, produced noticeably more symmetric exchange tensors — results that better respect the expected symmetry of the system and are markedly more robust to numerical noise in the DFT energies.

In parallel I completed a spin model of graphene triangulenes embedded in hexagonal boron nitride. Triangular nanographene fragments carry a net spin set by their sublattice imbalance (Lieb's theorem); embedded in an hBN matrix they form a lattice of localized moments whose mutual exchange, mediated by the surrounding carbon network, was extracted and assembled into an effective Heisenberg model with the same first-principles methodology. The work was presented at the DPG Spring Meeting (Regensburg), *Let's give it a spin!* (Belgrade) and CECAM (Toulouse).

The quantum reservoir computing (QRC) line also advanced: we used the nitrogen-vacancy (NV^-) center in diamond as a physical reservoir. A time series was encoded into the NV^- spin by a train of π pulses, and we then performed a virtual density-matrix tomography, so that *all* elements of the reconstructed density matrix were available as features for the machine-learning readout, rather than a single projected observable. Exploiting the full density matrix in this way, the reservoir could perform successive (multi-step-ahead) prediction of the time series far beyond what a simple linear fit of the same series achieves.

Semester 3: first applications and new directions

The third semester turned `grogupy` from a validated tool into a productive one and opened two further projects.

CrI_3/WTe_2. Following the monolayer and bilayer CrI_3 tests, we applied the full pipeline to CrI_3 proximity-coupled to metallic WTe_2. The relativistic exchange tensors were computed for the free and the proximity-coupled layer, revealing a longer-ranged isotropic exchange and a reorientation of the magnetic anisotropy on WTe_2; the finite-temperature consequences were then obtained by Monte Carlo. This established the first full physics application of the package (the detailed results are given in the next section). The study was coordinated with the Oviedo group (Z. Tajkov, J. Ferrer, A. García-Fuente) and with E. Navarro-Moratalla through recurring meetings.

V_B^- in hBN. Together with other ELTE PhD students, we set up the cluster-correlation expansion (CCE) framework, using `pyCCE`, to compute the coherence time of the spin-triplet boron-vacancy center. The effort this semester focused on building the central-spin-plus-bath model, assembling the spin-1/2, spin-1 and nuclear bath, and validating the CCE convergence with respect to cluster order, bath size, and the number of ensemble realizations, in preparation for the production runs of the following semester.

TFIM reservoir computing. With the Loughborough group I started a QRC study based on transverse-field Ising model (TFIM) reservoirs,

$$H_{\mathrm{TFIM}} = -J \sum_i \sigma_i^z \sigma_{i+1}^z - h \sum_i \sigma_i^x, \tag{5}$$

examining how the field ratio h/J — which drives the chain across its quantum phase transition — sets the trade-off between the reservoir's memory and its nonlinearity, building on the experience gained with the NV^- reservoir.

Research work carried out in the current semester

CrI_3/WTe_2: proximity-induced spin reorientation

This project was completed during the current semester and posted on arXiv.

Geometry and stacking. A commensurate CrI_3/WTe_2 supercell was constructed to accommodate the lattice mismatch of the two layers, whose primitive cells are mutually incommensurate; a commensurate approximant was built by lightly straining the layers onto a common periodicity chosen to minimize the residual strain while keeping the atom count tractable. After geometric relaxation, the relative lateral registry of the layers was optimized by a two-dimensional stacking scan at fixed interlayer separation, parametrized by the in-plane shift $\Delta\mathbf{r}_{xy} = s_a\,\mathbf{a} + s_b\,\mathbf{b}$; the total-energy map, sampled on a grid in (s_a, s_b) and interpolated to its minimum, selects the stacking $s_a = 1/6$, $s_b = -1/6$. The Cr $3d$ states were treated with a Hubbard correction, and the magnetic interactions were obtained from fully relativistic (spin–orbit) calculations.

Electronic structure. Isolated CrI_3 is a magnetic semiconductor (the monolayer orders experimentally near 45 K, about twice our computed value of $\sim$23 K). On WTe_2 it becomes metallic through charge equilibration across the interface, but its bands are otherwise essentially unperturbed: a layer-projected band structure shows the CrI_3- and WTe_2-derived states retaining their separate character around the Fermi level, with only the relative alignment shifted. There is no major electronic reconstruction, and the consequences for the magnetism are therefore a genuine relativistic proximity effect rather than a chemical one — this is the central physical point of the study.

Exchange interactions and reorientation. The isotropic exchange $J^{\mathrm{iso}}(d)$, resolved as a function of the Cr–Cr distance d, retains its short-range ferromagnetic nearest-neighbour coupling but acquires a noticeably longer range in the proximity-coupled case, reflecting an RKKY-like contribution mediated by the WTe_2 conduction electrons. The symmetric anisotropic exchange, resolved shell by shell, is redistributed in the outer shells, and summing the single-ion and two-site anisotropic contributions the magnetocrystalline anisotropy energy switches sign,

$$\Delta E = E_{\mathrm{IP}} - E_{\mathrm{OOP}} = \begin{cases} +0.94 \text{ meV/cell}, & \text{isolated } \mathrm{CrI_3} \text{ (OOP easy axis)}, \\ -0.35 \text{ meV/cell}, & \mathrm{CrI_3/WTe_2} \text{ (IP easy axis)}, \end{cases} \tag{6}$$

so that the easy axis rotates from out-of-plane (OOP) in the free layer to in-plane (IP) on WTe_2 (Fig. 1a) — a proximity-induced spin reorientation.

Finite-temperature magnetism. The extracted tensors were fed into large-scale VAMPIRE Monte Carlo simulations [**evans2014vampire**] of the relativistic Heisenberg model; for this step `grogupy` writes the full set of relativistic tensors directly into VAMPIRE input files for a large magnetic supercell, removing a tedious and error-prone manual step. From the reduced magnetization $m(T) = |\mathbf{M}(T)|/M_0$ and the magnetic susceptibility

$$\chi_m = \frac{1}{k_B T}\Big(\langle|\mathbf{M}|^2\rangle - \langle|\mathbf{M}|\rangle^2\Big), \tag{7}$$

the Curie temperature is identified from the peak of $\chi_m(T)$, giving a 40–50% enhancement on WTe_2 together with the easy-axis switch (Fig. 1b). The longer-ranged isotropic exchange and the reoriented anisotropy thus reinforce one another, both stabilizing magnetic order to higher temperature and rotating its preferred direction.

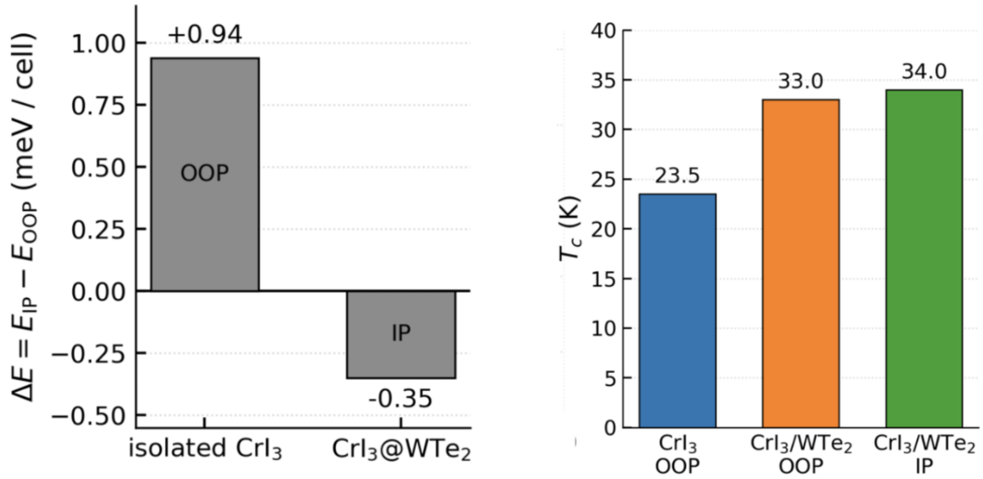

Figure 1: Proximity-induced changes in monolayer CrI_3 on WTe_2. (a) The magnetocrystalline anisotropy energy $\Delta E = E_{\mathrm{IP}} - E_{\mathrm{OOP}}$ switches sign, signalling the out-of-plane $\rightarrow$ in-plane easy-axis reorientation. (b) Curie temperatures from VAMPIRE Monte Carlo, showing the 40–50% enhancement on WTe_2.

V_B^- coherence in hBN

This project was completed in manuscript form (not yet posted on arXiv).

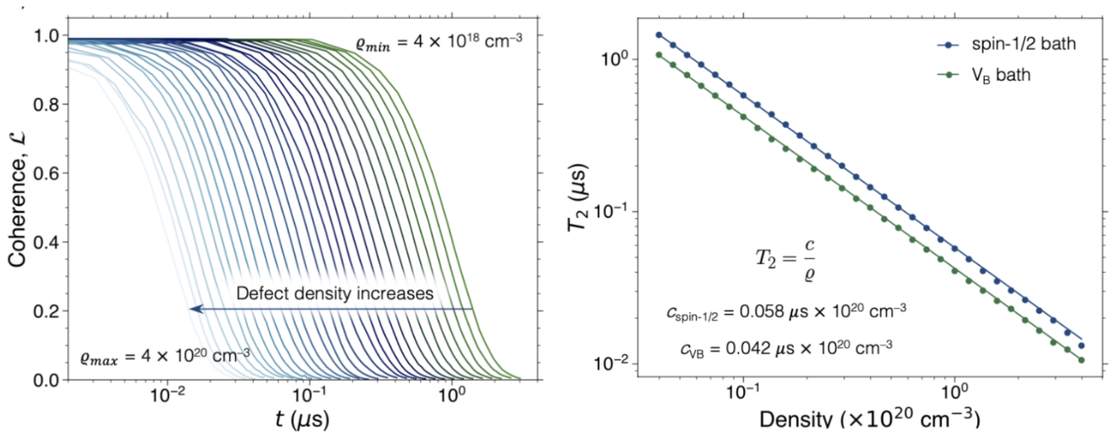

Figure 2: Coherence of the V_B^- center. (a) Ensemble-averaged spin-echo coherence $\mathcal{L}(t)$ for increasing defect density, each curve a stretched exponential. (b) The resulting coherence time follows an inverse-density law $T_2 = c/\varrho$ for both the spin-1/2 and the V_B bath.

The defect and its Hamiltonian. The negatively charged boron vacancy V_B^- in hBN is a spin-triplet ($S = 1$) color center; its electronic spin is governed by

$$H_{\mathrm{V}_B} = D\, S_z^2 + E\,(S_x^2 - S_y^2) + g\mu_B\, \mathbf{B}\cdot\mathbf{S}, \tag{8}$$

with axial and transverse zero-field-splitting parameters D and E. The full decoherence problem couples this central spin to a structured bath,

$$H = H_{\mathrm{V}_B} + H_{\mathrm{int}} + H_{\mathrm{bath}}, \qquad H_{\mathrm{bath}} \approx H_{\text{spin-1/2}} + H_{\text{spin-1}} + H_{\mathrm{nuc}}, \tag{9}$$

comprising electronic spin-1/2 and spin-1 defects together with the dense nuclear-spin background of the host.

Cluster-correlation expansion. The Hahn-echo coherence $\mathcal{L}(t) = \langle S_+(t)\rangle / \langle S_+(0)\rangle$ was evaluated in the CCE, in which the coherence factorizes into a product of irreducible cluster contributions,

$$\mathcal{L}(t) = \prod_C \tilde{\mathcal{L}}_C(t), \tag{10}$$

truncated at the pair level (CCE-2); the calculations were performed with `pyCCE`. Averaging over random spatial realizations of the bath yields the ensemble coherence (Fig. 2a), well described by the factorized, stretched-exponential form

$$\mathcal{L}(t) = \mathcal{L}_0\, f_{\mathrm{EEM}}(t) \prod_{b\,\in\,\{1/2,\,1,\,\mathrm{nuc}\}} \exp\left[-\left(\frac{t}{T_2^{(b)}}\right)^{n_b}\right], \tag{11}$$

where $f_{\mathrm{EEM}}(t)$ is the electron–electron-modulation envelope and n_b the per-species stretching exponents. At short times the coherence additionally carries electron-spin-echo envelope modulations (ESEEM) from the most strongly coupled nuclear spins, whose hyperfine coupling is spectrally resolved rather than motionally averaged; these appear as oscillations superimposed on the otherwise smooth stretched-exponential decay.

Bath-resolved behaviour. The spin-1/2 bath is dominated by Markovian noise, producing a nearly field-independent decay. The spin-1 bath, by contrast, causes stronger decoherence and faster precession; it additionally exhibits the characteristic ground-state level anticrossing (GSLAC), where the $|0\rangle$ and $|-1\rangle$ sublevels of the $S = 1$ manifold approach degeneracy when the Zeeman energy matches the zero-field splitting,

$$B_{\mathrm{GSLAC}} = \frac{hD}{g\mu_B} \approx 125\ \mathrm{mT} \quad (D \approx 3.5\ \mathrm{GHz}), \tag{12}$$

producing a sharp feature in the coherence and in the fitted exponent near that field. Because real samples contain many defects, the simulations also treated the coupled two-defect case: two exchange- and dipolar-coupled V_B^- centers form a two-qubit manifold whose joint levels $|00\rangle\,, |0\,{-1}\rangle\,/\,|{-1}\,0\rangle\,, |{-1}\,{-1}\rangle\,, \ldots$ disperse with the applied field and cross near the GSLAC, opening additional flip-flop channels that modify the effective bath seen by each central spin.

Density and thickness scaling. Ensemble-averaged calculations reveal a clean inverse-density scaling of the coherence time (Fig. 2b),

$$T_2 = \frac{c}{\varrho}, \qquad c_{\text{spin-1/2}} = 0.058, \quad c_{\mathrm{V}_B} = 0.042\ \ \mu\mathrm{s}\cdot 10^{20}\,\mathrm{cm}^{-3}, \tag{13}$$

and a sample-thickness dependence

$$T_2 \approx T_{2,\varrho} + a\left(\frac{d_3}{d}\right)^{1.6}, \qquad a_{\text{spin-1/2}} = 0.026, \quad a_{\mathrm{V}_B} = 0.019\ \ \mu\mathrm{s}. \tag{14}$$

The thickness law describes the crossover from a three-dimensional bath (thick samples) to a quasi-two-dimensional one (thin flakes) and shows that thinning the sample substantially lengthens T_2 — a result of direct relevance to the design of hBN-based quantum sensors. Beyond the single-pulse Hahn echo, the same framework was applied to multi-pulse dynamical-decoupling sequences (CPMG- and XY-type), which act as a tunable band-pass filter on the bath noise spectrum: increasing the number of refocusing pulses suppresses the low-frequency components of the noise and progressively extends the coherence, the gain being largest against the slowly fluctuating nuclear bath.

Outlook

grogupy is now being applied to new systems, including yttrium iron garnet (YIG) and $NiBr_2$, to test the method across very different magnetic materials and to support the experimental and theoretical partners in the consortia. In parallel I am pursuing a separate quantum-reservoir-computing project on quantum state recognition, using a Trotterized in-plane-magnetized Ising model as the reservoir, together with two PhD students from ELTE. Both lines, together with the journal publication of the two manuscripts described above, define the immediate continuation of the work.

Studies in current semester

- Sensory Biophysics II (FIZ/3/045E) — Excellent.
- Quantum Computer Science (FIZ/3/100) — Satisfactory.
- Quantum Information Theory (FIZ/1,3/060E) — Good.

Conferences during the doctoral training

1. 8th Graphene and 2D Materials Workshop — BME, Budapest, 18–20 Sep 2024.
2. TRILMAX kickoff meeting — ELTE, Budapest, 25–28 Sep 2024.
3. QUEST kickoff meeting — ELTE, Budapest, autumn 2024.
4. *Advancing Quantum Theory for Future Quantum Technologies* — Linköping University, Sweden, 17–24 Nov 2024.
5. QRC consortium kick-off — ELTE, Budapest, 28–31 Jan 2025.
6. DPG Spring Meeting (Condensed Matter) — Regensburg, 15–22 Mar 2025 — **contributed talk (MA 8.6)**.
7. COST CA23134 “Polytopo” — BME, Budapest, 14–16 May 2025.
8. *Let’s give it a spin!* — Belgrade, 20–23 May 2025 — **oral talk**.
9. CECAM conference — Toulouse, 24–28 Jun 2025 — **poster**.
10. Valencia laboratory visit ($NiBr_2$) — Valencia, 14–27 Jul 2025.
11. Aalto/Helsinki Summer School (Quantum and Quantum Reservoir Computing) — Aalto, Finland, 18–23 Aug 2025.
12. TRILMAX Theory Summer School — Oviedo, Spain, 7–12 Sep 2025 — **invited tutor**.
13. Loughborough research stay — 28 Sep – 1 Nov 2025.
14. Loughborough research stay — 1 Feb – 15 Mar 2026.
15. APS March Meeting — Denver, USA, March 2026 — **talk** (CrI_3/WTe_2 + grogupy).

16. Intermag 2026 — Manchester, UK, 12–17 Apr 2026 — **talk** (same contribution).

Throughout the training I also attended weekly group meetings and journal clubs at ELTE, and theory meetings within the QUEST and TRILMAX consortia.

Patents

All three of the following are currently pending — two filed through the ELTE Innovation Office and one disclosed at Aalto University:

- Room-temperature quantum reservoir computing with optically addressable paramagnetic defects (ELTE).
- Sensing with a quantum reservoir in condensed matter (ELTE).
- Optimal quantum circuit for quantum machine learning (Aalto).

Teaching activity

- Semester 1 — Data Mining and Machine Learning: project supervision and final-report grading (FIZ/OKT/2, completed).
- Semester 2 — Numerical Methods in Physics: exercise instructor (not separately credited).
- Semester 3 — Computer Science Fundamentals: exercise instructor (FIZ/OKT/2, completed).
- Semester 4 — Numerical Methods in Physics: exercise instructor (FIZ/OKT/4, in progress).

Acknowledgments

This research has been made possible through the support of two Horizon Europe projects, QUEST and TRILMAX. These initiatives have provided invaluable opportunities for conference attendance and professional development within a collaborative research environment. I gratefully acknowledge the computational resources provided by KIFÜ in Hungary and NAISS in Sweden, which have been essential for conducting our numerical simulations and analyses.

References

[1] Gabriel Martínez-Carracedo et al. "Relativistic magnetic interactions from nonorthogonal basis sets". In: *Physical Review B* 108.21 (2023), p. 214418.